

Presaturation phase with no dipolar order in a quantum ferro-antiferromagnet

V. K. Bhartiya,^{1,*} K. Yu. Povarov,¹ D. Blosser,¹ S. Bettler,¹ Z. Yan,¹ S. Gvasaliya,¹ S. Raymond,² E. Ressouche,² K. Beauvois,³ J. Xu,⁴ F. Yokaichiya,⁴ and A. Zheludev^{1,†}

¹Laboratory for Solid State Physics, ETH Zürich, 8093 Zürich, Switzerland

²Univ. Grenoble Alpes, CEA, IRIG/DEPHY/MEM-MDN, F-38000 Grenoble, France

³Institut Laue Langevin, 38000 Grenoble, France

⁴Helmholtz-Zentrum Berlin für Materialien und Energie GmbH,
Hahn-Meitner-Platz 1, D-14109 Berlin, Germany

(Dated: January 22, 2022)

Magnetization, magnetocaloric, calorimetric, neutron and X-ray diffraction and inelastic neutron scattering measurements are performed on single crystals of $\text{BaCdVO}(\text{PO}_4)_2$. The low-temperature crystal structure is found to be of a lower symmetry than previously assumed. The result is a more complicated model spin Hamiltonian, which we infer from measurements of the spin wave dispersion spectrum. The main finding is a novel spin state which emerges in high magnetic fields after antiferromagnetic order is terminated at $H_{c1} \simeq 4.0$ T. It is a distinct thermodynamic phase with a well-defined phase boundary at $H_{c2} \simeq 6.5$ T and is clearly separate from the fully saturated phase. Yet, it shows no conventional (dipolar) magnetic long range order. We argue that it is fully consistent with the expectations for a quantum bond-nematic state.

Conventional long range order in spin systems is represented by a static, usually periodically modulated magnetization. It breaks both rotational and time-reversal symmetries of the underlying Heisenberg Hamiltonian. Spin nematic order, as first envisioned by M. Blume [1] and generalized by A. F. Andreev [2], breaks rotational but not time reversal symmetries. Spins continue to fluctuate, but these fluctuations *spontaneously* become anisotropic. From a theorist's perspective such exotic quantum states are robust and not particularly rare, often realized in partially magnetized systems with competing antiferromagnetic (AF) and ferromagnetic (FM) interactions [3–5]. For example, the simple next-nearest-neighbor (nnn) Heisenberg AF on a square lattice with nearest-neighbor (nn) FM coupling is predicted to always be a spin nematic in some range of applied magnetic fields just below full polarization (FP) [6, 7]. Finding an experimental realization of even this relatively unconstrained model is a formidable challenge. The only known potential host compounds are layered vanadophosphates of type $AA'\text{VO}(\text{PO}_4)_2$ [8, 9]. Until recently, no unambiguous signatures of spin nematic phases have been found in any of them. The main obstacle has been a lack of single crystal samples. Indeed, powder data are notoriously difficult to interpret. In applied magnetic fields, where each crystallite experiences *a priori* different conditions, phase transitions and other anomalies that may be indicative of the nematic state become washed out. Thus, single crystal experiments are key.

In our recent paper [10] we reported the first thermodynamic evidence of a novel presaturation quantum phase in small single crystals of $\text{BaCdVO}(\text{PO}_4)_2$, one of the most promising host materials [11]. Powder magnetometric and neutron diffraction studies by other authors [12] seemingly supported the notion of the new phase being the elusive spin nematic state, but, as ar-

gued below, may otherwise be misleading. In the present work we settle this issue decisively. We report combined neutron and X-ray diffraction, inelastic neutron scattering, Faraday balance magnetometry, calorimetry and magnetocaloric(MCE) studies on appropriate size $\text{BaCdVO}(\text{PO}_4)_2$ *single crystals*. We first show that the low-temperature crystallographic structure is of a lower symmetry than previously assumed. Consequently, the spin wave spectrum is quite different from that of a simple square lattice. Despite that, the putative pre-saturation nematic phase exists and persists over a surprisingly wide range of applied magnetic fields. It has distinct thermodynamic phase boundaries, but its polarization is almost complete, over 98% of full saturation.

At room temperature $\text{BaCdVO}(\text{PO}_4)_2$ has an orthorhombic P_{bca} (D_{2h}^{15} , No. 61) structure with 8 V^{4+} ions per unit cell [13] forming an approximate $S = 1/2$ square lattice in the (a, b) plane. If what is known about the structurally similar $\text{Pb}_2\text{VO}(\text{PO}_4)_2$ is any guidance [14], magnetic interactions are in the these planes, with negligible inter-layer coupling. The nn and nnn in-plane exchange constants for $\text{BaCdVO}(\text{PO}_4)_2$ have been previously estimated from powder data as $J_1 = -0.31$ and $J_2 = 0.28$ meV [15]. There is also a weak easy-axis anisotropy that manifests in a spin flop transition (SF) around $\mu_0 H_{\text{SF}} \simeq 0.5$ T for $\mathbf{H} \parallel \mathbf{a}$ [10].

Long range magnetic order in zero applied field is of a peculiar “up-up-down-down” type, propagation vector $(0, 1/2, 0)$, and appears below $T_N = 1.05$ K [12]. It is incompatible with the simple J_1 - J_2 model and was attributed to additional 3rd-nearest neighbor (3nn) interactions in the V^{4+} layers [12, 16]. There is, however, a more natural explanation. It turns out that $\text{BaCdVO}(\text{PO}_4)_2$ undergoes a structural phase transition at $T \sim 250$ K. It was detected by tracking the temperature dependence of the $(0, -3, -7)$ neutron Bragg reflection with CRG-D23

diffractometer at ILL. This Bragg reflection is forbidden in P_{bca} but becomes visible below the transition point (see supplementary material). At low temperature the compound remains orthorhombic with the reduced space group $P_{ca}2_1$ (C_{2v}^5 , No. 29). The structure was solved at $T = 120$ K from 14519 Bragg peak intensities collected in a single crystal X-ray diffraction experiment using a Bruker APEX-II diffractometer. Details of the crystallographic refinement are reported in the supplement. The $P_{ca}2_1$ structure, with two inequivalent V^{4+} positions, allows for as many as 4 nn and 4 nnn interactions within each V^{4+} layer as shown in the inset of Fig. 1. In particular, unlike at room temperature, there is a possibility of alternating nn and nnn interactions along the crystallographic b axis. This naturally explains the $(0, 1/2, 0)$ magnetic propagation vector without invoking 3nn coupling, which would have to span over an unrealistic 8 Å distance.

To elucidate the effect of lowered crystal symmetry on the coupling constants in $BaCdVO(PO_4)_2$ we performed preliminary inelastic neutron scattering measurements of the spin wave (SW) dispersion in the fully saturated phase. The data were collected at $T = 70$ mK on the IN12 cold neutron 3-axis spectrometer at CRG-ILL in an $\mu_0 H = 10$ T magnetic field applied along the crystallographic c axis. We co-aligned two crystals of total mass 320 mg and a combined mosaic of 10° full width at half height grown using 98.8% isotopically enriched ^{144}Cd to reduce neutron absorption. A series of constant- Q scans performed with 3.5 meV final energy neutrons (see supplement) reveal the dispersion relations plotted in Fig. 1 (symbols). It was analyzed using linear spin wave theory (SPINW package [17]). The entire set of eight exchange constants can *not* be uniquely determined from the three sets of measured dispersion curves. However, we find that without an alternation of J s along the b direction the two distinct spin wave branches clearly visible in the data can not be accounted for. With such an alternation, even a restricted minimal model reproduces the measured spectrum reasonable well with $J_1^a = J_1'^a = J_1^b = -0.42$, $J_1'^b = -0.34$, $J_2^+ = J_2^- = 0.16$ and $J_2'^+ = J_2'^- = 0.38$ meV. The corresponding calculated scattering intensities [17] are shown as a false color plot in Fig. 1. Further measurements will be needed to uniquely determine the Hamiltonian, but it is already clear that for $BaCdVO(PO_4)_2$ the simple J_1 - J_2 model is inadequate and that an alternation of exchange constants plays a crucial role.

We now turn to the main focus of the present paper, which is the putative low-temperature nematic phase (LT) in applied fields. It emerges at $\mu_0 H_{c1} \simeq 4$ T in either a first- or second-order transition for $\mathbf{H} \parallel \mathbf{a}$ and $\mathbf{H} \parallel \mathbf{b}$, respectively [10]. The problem with the nematic order parameter is that it is *not directly accessible* to any experimental technique [18]. The only way to identify it is thus by a combination of complementary measure-

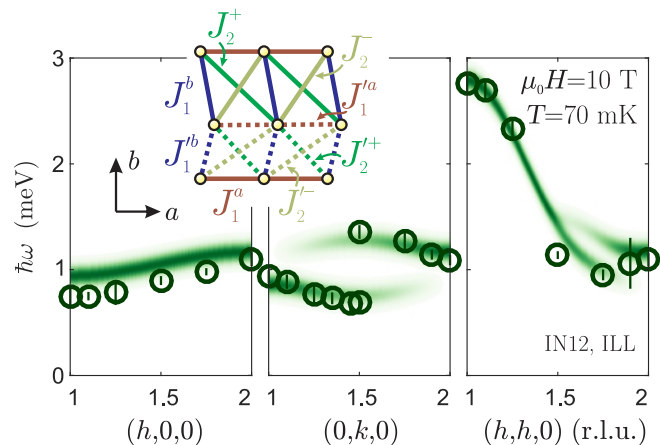


FIG. 1. Spin wave spectrum in fully polarized $BaCdVO(PO_4)_2$. Symbols are experimental data, the shading in the background shows the intensities from linear spin wave theory. Inset: schematic of symmetry-allowed Heisenberg exchange interactions in the $P_{ca}2_1$ structural phase of $BaCdVO(PO_4)_2$.

ments. Figures 2 and 3 show such data for two sample geometries, with the magnetic field applied parallel and perpendicular to the magnetic easy axis, respectively. All these measurements are carried out at base temperatures of 3He - 4He dilution refrigerators (100 mK or lower) on single crystals grown as described in Ref. [10].

Exhibit one (top panels in Figs. 2 and 3) is heat capacity measured vs. applied magnetic field using a commercial Quantum Design PPMS relaxation calorimetry setup on a 2.3 mg crystal of $BaCdVO(PO_4)_2$. As described in detail in Ref. [10], for $\mathbf{H} \parallel \mathbf{a}$, the discontinuous spin flop transition at $\mu_0 H_{SF}$ and another one at $\mu_0 H_{c1} = 4.00(5)$ T are marked by sharp steps in the heat capacity. For $\mathbf{H} \parallel \mathbf{c}$ there is no spin flop transition and the specific heat exhibits a strong divergence approaching $\mu_0 H_{c1} = 4.08(5)$ T. In both cases, fluctuations persist above $\mu_0 H_{c1}$, marking the novel pre-saturation state. In all the orientations the specific heat plateau above $\mu_0 H_{c1}$ visibly collapses around a crossover field $\mu_0 H_* \simeq 5.5$ T. This pronounced change in the resulting specific heat stems from an onset of “temperature arrest” kind of behavior in the relaxation curves. We interpret it as a hint of the phase separation taking place in the sample [19, 20]. At any orientation at still higher field $\mu_0 H_{c2} \simeq 6.5$ T there clearly is an additional lambda anomaly, albeit a weak one [21].

The transition at H_{c2} is even more obvious in exhibit two [panels (b) in Figs. 2 and 3]. These are magnetocaloric measurements on the same sample using a constant field sweep rate of 1 mT/sec. Up and down sweeps are shown as darker and lighter lines, respectively. For $\mathbf{H} \parallel \mathbf{a}$ at around 130 mK, H_{SF} and H_{c1} are both marked by asymmetric anomalies, characteristic of discontinuous transitions [22]. For $\mathbf{H} \parallel \mathbf{c}$ the lowest-temperature mag-

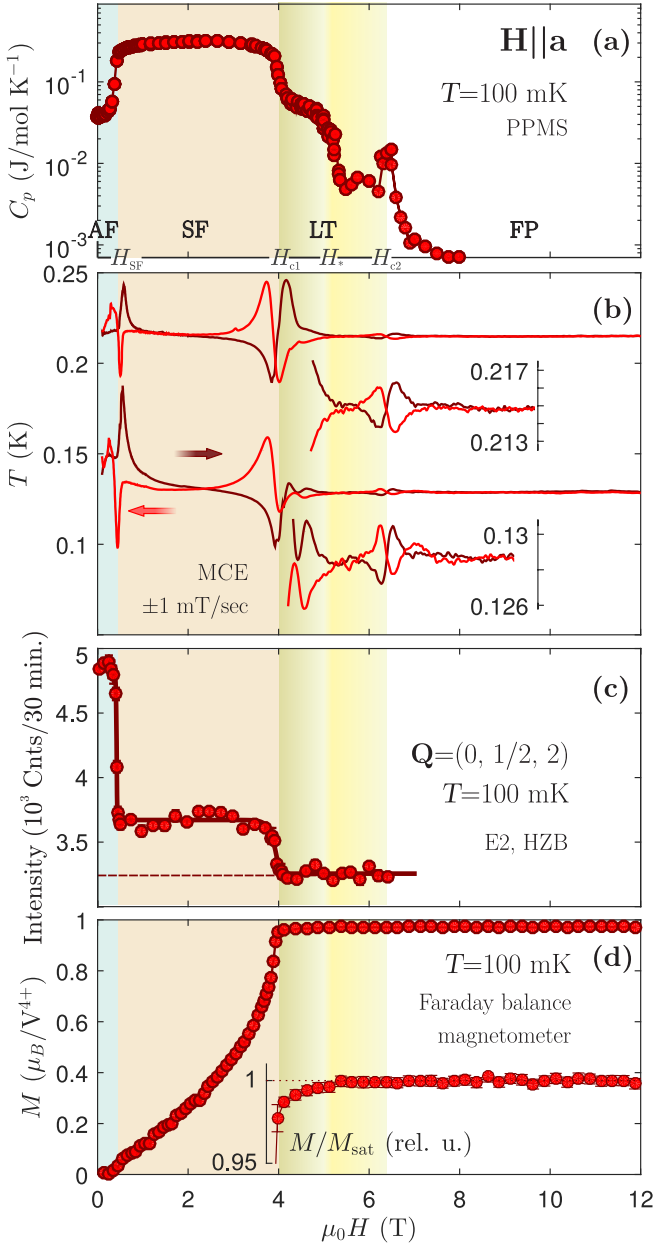


FIG. 2. Magnetic thermodynamics of $\text{BaCdVO}(\text{PO}_4)_2$ single crystals in the axial $\mathbf{H} \parallel \mathbf{a}$ geometry. (a) Specific heat at 100 mK. (b) Magnetocaloric effect measurements at 130 and 215 mK. The insets show the fine structure of $T(H)$ curves above H_{c1} in more detail. (c) Neutron diffraction intensity at the $(0, 1/2, 2)$ magnetic Bragg peak position at 100 mK. The solid line is a guide to the eye, the dashed line shows the background intensity. (d) Magnetization curve at 100 mK. The inset shows a zoomed-in structure of M/M_{sat} curve above H_{c1} .

netocaloric sweeps the anomaly at H_{c1} is also asymmetric. At the same time, a weak but clear magnetocaloric anomaly is also present at H_{c2} for all the orientations. At slightly elevated temperatures [$T \simeq 210$ mK set of curves in Figs. 2(b) and 3(b)] the main anomaly at H_{c1}

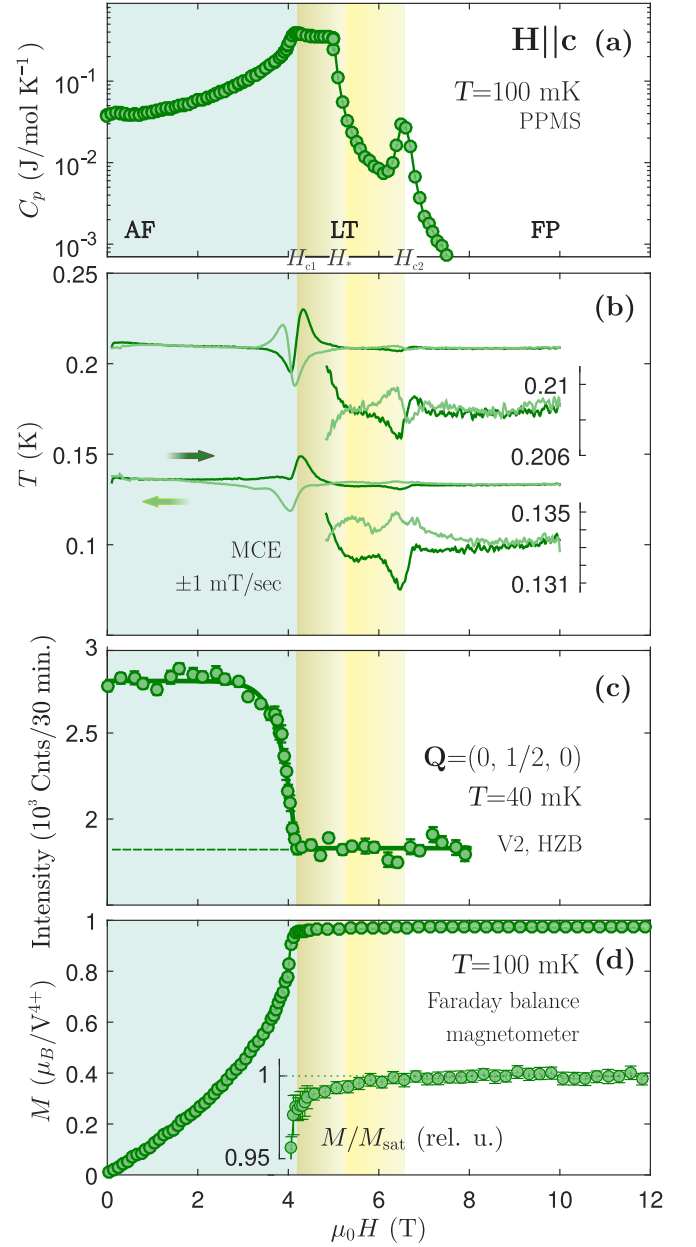


FIG. 3. Similar measurements in the transverse $\mathbf{H} \parallel \mathbf{c}$ geometry. (c) shows the field dependence of the $(0, 1/2, 0)$ magnetic Bragg peak at 40 mK.

turns symmetric, indicative of a continuous phase transition [22]. In both geometries, at slightly elevated temperatures the transition at H_{c2} is clearly continuous as well.

Additional magnetocaloric effect scans at different temperatures allow us to trace the H_{c2} phase boundary vs. temperature and reconstruct the $H - T$ phase diagram. The transition can be followed up to about 500 mK. Up to 350 mK it barely shifts and shows no sign of broadening: only its magnitude decreases. Above 350 mK the left shoulder of the magnetocaloric anomaly

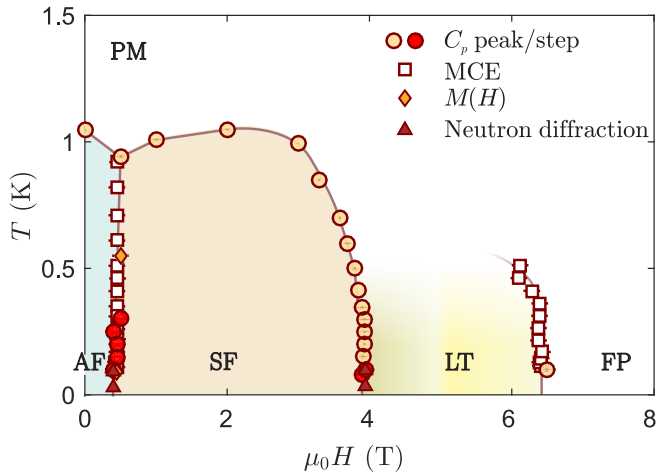


FIG. 4. Magnetic phase diagram of $\text{BaCdVO}(\text{PO}_4)_2$ for $\mathbf{H} \parallel \mathbf{a}$ field direction obtained by a combination of measurement techniques. Solid lines are guide to the eye. The phases are: PM and FP — paramagnet and fully polarized paramagnet, AF and SF — conventional antiferromagnetic states before and after spin-flop, LT — novel presaturation phase presumed to be the quantum spin nematic state.

vanishes and it turns into a broad peak. This peak becomes indiscernible in the data noise above 500 mK. Fig. 4 shows the phase boundaries deduced from MCE, magnetization, neutron diffraction, and specific heat [10]. Very similar temperature-dependent behavior was observed for $\mathbf{H} \parallel \mathbf{c}$ and $\mathbf{H} \parallel \mathbf{b}$ (not shown). The measured phase diagram for $\text{BaCdVO}(\text{PO}_4)_2$ shows certain similarities to the one recently reported for volbortite, a very complicated frustrated magnet that is to some extent equivalent to a $S = 1/2$ model on a frustrated square lattice and also expected to host a spin nematic phase [23].

Which of the transitions observed in $\text{BaCdVO}(\text{PO}_4)_2$ corresponds to a destruction of conventional long range order? This is clarified by exhibit 3 [panels (c) in Figs. 2 and 3], which shows the field dependence of the magnetic Bragg peaks $(0, 1/2, 2)$ and $(0, 1/2, 0)$ measured via neutron diffraction. These data were taken on the V2 [Fig. 3(c)] and E2 [Fig. 2c] instruments at the BER reactor at HZB using 2.74 meV and 14.2 meV neutrons and 142 and 24 mg ^{144}Cd -enriched single crystals, respectively. In both geometries the disappearance of conventional magnetic order exactly coincides with $\mu_0 H_{c1}$. That no magnetic structure with a different propagation vector exists in higher fields is clear from powder diffraction experiments of Ref. [12]. We thus identify the region $H > H_{c2}$ as fully saturated and the field range $H_{c1} < H < H_{c2}$ as corresponding to the potential spin-nematic phase.

Of course, this interpretation implies that for $H_{c1} < H < H_{c2}$ the system does *not* achieve full polarization. Exhibit 4 (inset of panels (d) in Figs. 2 and 3) puts this supposition to the test. These are direct Faraday force

measurements of magnetization at $T = 100$ mK from a 0.8 mg sample. A small diamagnetic linear contribution was inferred from measurements above 8 T and subtracted from the data shown. For both geometries, the data show a divergent magnetic susceptibility at H_{c1} , seemingly followed by a complete saturation above. The blow-up of the high-field region shown in the insets in Figs. 2 and 3 reveal a different story. In order to reduce noise, the data for $\mu_0 H > 4$ T were binned together in 0.25 T intervals. Between $\mu_0 H_{c1}$ and at least 5.5 T the magnetization visibly lies *below* the average value for all data above 8 T (dashed line). The effect is small but clearly outside of the measurement uncertainty represented by the error bars.

Incomplete polarization at high field could in principle stem from the small magnetic anisotropy present in the system [24, 25]. However, this scenario can be excluded. The effect would have to be absent in the axial geometry, and in all cases confined to a much narrower field range, comparable to the spin flop field value [25]. The high field phase is indeed *not* fully saturated. At the same time its polarization is in all cases over 98%. Can such a highly polarized state support nematic order? Arguably it can, since the latter involves *transverse* spin components [6, 11]. As a reference, consider a classical AF at 99% saturation. Despite being almost fully polarized it will still have an angle of as much as 16° between consecutive spins, sufficient for AF order of transverse spin components. Similarly, such proximity to saturation leaves ample room for nematic correlations in the transverse channel.

There are stark discrepancies between our results and the powder measurements of Ref. [12]. In that work the magnetization curves were obtained by integrating AC susceptibility data. The one corresponding to the lowest experimental temperature $T = 200$ mK is considerably less inflected below H_{c1} than our curves shown in Figs. 2(d) and 3(d) or even those previously measured at $T = 550$ mK [10]. The inflection point that the authors take for the analogue of H_{c1} doesn't correspond to any features in our data for any field geometry. The reported value $\mu_0 H_{c1} = 3.78$ T is considerably lower than $\mu_0 H_{c1} \gtrsim 4.0$ T observed in single crystals for *all* geometries. The huge reduction of magnetization in the high-field phase concluded in Ref. [12] is most certainly due to H_{c1} being underestimated.

The upper boundary assigned to the nematic phase in Ref. [12] does not correspond to any thermodynamic anomalies in single crystals. Counter-intuitively it moves out to higher fields with increased temperature. As is quite obvious from previously published single crystal data [10], this simply indicates a broadening of the cusp in magnetization due to finite temperature. Our present data instead suggest that the upper phase boundary is more or less parallel to the lower one, as one would expect. We cannot speculate on the origin of these discrep-

ancies, except to note the intrinsic limitations of powder experiments in applied field and the difficulties of dealing with a dissipative component in AC susceptibility admitted by the authors of Ref. [12].

In summary, $\text{BaCdVO}(\text{PO}_4)_2$ is *not* a square lattice model material as it was advertised to be. Instead, it has significantly alternating interactions along the b direction. Nevertheless, it features strong FM-AFM frustration, the main ingredient for a pre-saturation bond-nematic phase. While the corresponding order parameter is fundamentally inaccessible to direct measurements, at the lowest temperatures, in a wide field range between $\mu_0 H_{c1} \simeq 4.0$ T and $\mu_0 H_{c2} \simeq 6.5$ T we find a novel *almost* fully polarized thermodynamic phase. It does not support conventional (dipolar) magnetic order but is fully consistent with our expectations for a quantum bond-nematic.

This work was supported by the Swiss National Science Foundation, Division II. The instrument beamtime at D23 and IN12 was supported by the Swiss State Secretariat for Education, Research and Innovation (SERI) through a CRG Grant. We would like to acknowledge Dr. M. Reehius at HZB for his help with checking single crystals quality as well as the sample environment team of the ILL facility for their help with our experiments.

* vvivek@phys.ethz.ch

† zhelud@ethz.ch; <http://www.neutron.ethz.ch/>

- [1] M. Blume and Y. Y. Hsieh, “Biquadratic Exchange and Quadrupolar Ordering,” *J. Appl. Phys.* **40**, 1249 (1969).
- [2] A. F. Andreev and I. A. Grishchuk, “Spin nematics,” *Sov. Phys. JETP* **60**, 267 (1984).
- [3] J. Sudan, A. Lüscher, and A. M. Läuchli, “Emergent multipolar spin correlations in a fluctuating spiral: The frustrated ferromagnetic spin- $\frac{1}{2}$ Heisenberg chain in a magnetic field,” *Phys. Rev. B* **80**, 140402 (2009).
- [4] M. E. Zhitomirsky and H. Tsunetsugu, “Magnon pairing in quantum spin nematic,” *Europhys. Lett.* **92**, 37001 (2010).
- [5] L. Balents and O. A. Starykh, “Quantum Lifshitz Field Theory of a Frustrated Ferromagnet,” *Phys. Rev. Lett.* **116**, 177201 (2016).
- [6] N. Shannon, T. Momoi, and P. Sindzingre, “Nematic order in square lattice frustrated ferromagnets,” *Phys. Rev. Lett.* **96**, 027213 (2006).
- [7] H. T. Ueda, “Magnetic Phase Diagram Slightly below the Saturation Field in the Stacked $J_1 - J_2$ Model in the Square Lattice with the J_C Interlayer Coupling,” *J. Phys. Soc. Jpn.* **84**, 023601 (2015).
- [8] A. A. Tsirlin and H. Rosner, “Extension of the spin- $\frac{1}{2}$ frustrated square lattice model: The case of layered vanadium phosphates,” *Phys. Rev. B* **79**, 214417 (2009).
- [9] A. A. Tsirlin, B. Schmidt, Y. Skourski, R. Nath, C. Geibel, and H. Rosner, “Exploring the spin- $\frac{1}{2}$ frustrated square lattice model with high-field magnetization studies,” *Phys. Rev. B* **80**, 132407 (2009).
- [10] K. Yu. Povarov, V. K. Bhartiya, Z. Yan, and A. Zheludev, “Thermodynamics of a frustrated quantum magnet on a square lattice,” *Phys. Rev. B* **99**, 024413 (2019).
- [11] A. Smerald, H. T. Ueda, and N. Shannon, “Theory of inelastic neutron scattering in a field-induced spin-nematic state,” *Phys. Rev. B* **91**, 174402 (2015).
- [12] M. Skoulatos, F. Rucker, G. J. Nilsen, A. Bertin, E. Pomjakushina, J. Ollivier, A. Schneidewind, R. Georgii, O. Zaharko, L. Keller, Ch. Rüegg, C. Pfleiderer, B. Schmidt, N. Shannon, A. Kriele, A. Senyshyn, and A. Smerald, “Putative spin-nematic phase in $\text{BaCdVO}(\text{PO}_4)_2$,” *Phys. Rev. B* **100**, 014405 (2019).
- [13] S. Meyer, B. Mertens, and Hk. Müller-Buschbaum, “ $\text{SrZnVO}(\text{PO}_4)_2$ and $\text{BaCdVO}(\text{PO}_4)_2$: Vanadylphosphates Related to but not Isotypic with the $\text{BaZnVO}(\text{PO}_4)_2$ Type,” *Z. Naturforsch.* **52b**, 985 (1997).
- [14] S. Bettler, F. Landolt, Ö. M. Aksoy, Z. Yan, S. Gvasaliya, Y. Qiu, E. Ressouche, K. Beauvois, S. Raymond, A. N. Ponomaryov, S. A. Zvyagin, and A. Zheludev, “Magnetic structure and spin waves in the frustrated ferro-antiferromagnet $\text{Pb}_2\text{VO}(\text{PO}_4)_2$,” *Phys. Rev. B* **99**, 184437 (2019).
- [15] R. Nath, A. A. Tsirlin, H. Rosner, and C. Geibel, “Magnetic properties of $\text{BaCdVO}(\text{PO}_4)_2$: A strongly frustrated spin- $\frac{1}{2}$ square lattice close to the quantum critical regime,” *Phys. Rev. B* **78**, 064422 (2008).
- [16] P. Sindzingre, L. Seabra, N. Shannon, and T. Momoi, “Phase diagram of the spin- $1/2$ $J_1 - J_2 - J_3$ Heisenberg model on the square lattice with ferromagnetic J_1 ,” *J. Phys.: Conf. Ser.* **145**, 012048 (2009); P. Sindzingre, N. Shannon, and T. Momoi, “Phase diagram of the spin- $1/2$ $J_1 - J_2 - J_3$ Heisenberg model on the square lattice,” *J. Phys.: Conf. Ser.* **200**, 022058 (2010).
- [17] S. Toth and B. Lake, “Linear spin wave theory for single- Q incommensurate magnetic structures,” *J. Phys.: Condens. Matter* **27**, 166002 (2015).
- [18] In principle, it can be probed with resonant magnetic X-ray diffraction. Unfortunately, this technique is incompatible with the high magnetic fields and mK temperatures at which the nematic state occurs in $\text{BaCdVO}(\text{PO}_4)_2$.
- [19] S. Röfler, D. Cherian, W. Lorenz, M. Doerr, C. Koz, C. Curfs, Yu. Prots, U. K. Röfler, U. Schwarz, Suja Elizabeth, and S. Wirth, “First-order structural transition in the magnetically ordered phase of $\text{Fe}_{1.13}\text{Te}$,” *Phys. Rev. B* **84**, 174506 (2011).
- [20] H. T. Ueda and T. Momoi, “Nematic phase and phase separation near saturation field in frustrated ferromagnets,” *Phys. Rev. B* **87**, 144417 (2013).
- [21] In both orientations the relaxation curves for $H > H_*$ were taken with ~ 30 sec. pulse length and interpreted within a simple exponential relaxation (single τ) model.
- [22] Y. Kohama, C. Marcenat, T. Klein, and M. Jaime, “AC measurement of heat capacity and magnetocaloric effect for pulsed magnetic fields,” *Rev. Sci. Instr.* **81**, 104902 (2010).
- [23] Y. Kohama, H. Ishikawa, A. Matsuo, K. Kindo, N. Shannon, and Z. Hiroi, “Possible observation of quantum spin-nematic phase in a frustrated magnet,” *Proc. Natl. Acad. Sci. U.S.A.* **116**, 10686 (2019).
- [24] R. Hagemans, J.-S. Caux, and U. Löw, “Gapped anisotropic spin chains in a field,” *Phys. Rev. B* **71**, 014437 (2005).

- [25] A. L. Chernyshev, “Effects of an external magnetic field on the gaps and quantum corrections in an ordered Heisenberg antiferromagnet with Dzyaloshinskii-Moriya anisotropy,” *Phys. Rev. B* **72**, 174414 (2005).

Supplemental material for “Presaturation phase with no dipolar order in a quantum ferro-antiferromagnet”

V. K. Bhartiya,^{1,*} K. Yu. Povarov,¹ D. Blosser,¹ S. Bettler,¹ Z. Yan,¹ S. Gvasaliya,¹ S. Raymond,² E. Ressouche,² K. Beauvois,³ J. Xu,⁴ F. Yokaichiya,⁴ and A. Zheludev^{1,†}

¹Laboratory for Solid State Physics, ETH Zürich, 8093 Zürich, Switzerland

²Univ. Grenoble Alpes, CEA, IRIG/DEPHY/MEM-MDN, F-38000 Grenoble, France

³Institut Laue Langevin, 38000 Grenoble, France

⁴Helmholtz-Zentrum Berlin für Materialien und Energie GmbH, Hahn-Meitner-Platz 1, D-14109 Berlin, Germany

(Dated: January 22, 2022)

I. STRUCTURAL PHASE TRANSITION

As mentioned in the main text, a smoking gun evidence for the lowered symmetry of $\text{BaCdVO}(\text{PO}_4)_2$ at low temperatures is the emergence of nominally extinct nuclear Bragg peaks around 250 K. An example of the temperature dependence of the $(0, -3, -7)$ nuclear peak measured via neutron diffraction is shown in Fig. 1. This data was measured on the CRG-D23 diffractometer at ILL on a 42 mg sample installed in a ^4He Orange cryostat. Neutrons with $k = 2.6 \text{ \AA}^{-1}$ were used. The observed temperature dependence is suggestive of crystal symmetry reduction.

We have solved the crystallographic structure of $\text{BaCdVO}(\text{PO}_4)_2$ at $T = 120 \text{ K}$ and indeed found it to be lower than P_{bca} . The low temperature structure corresponds to orthorhombic $P_{ca}2_1$ No. 29, a descendant of the original orthorhombic P_{bca} No. 61. The data (14519 reflections total) were obtained on a Bruker SMART-II single crystal X-ray diffractometer using a Mo-source and treated with the Bruker AXS software. Structure refinements were performed with SHELX. The results are presented in Table I. The listed values correspond to R -factors $R = 0.054$, and $wR = 0.16$.

One should also note that in $P_{ca}2_1$ notation (“dashed” axes given in Table I) the a and c axis are swapped with respect to P_{bca} notation. Nonetheless, for consistency with the previous work on $\text{BaCdVO}(\text{PO}_4)_2$ we keep referring to c as the longest and to a as the shortest axes. These are the axes non-dashed labels in Table I.

II. INELASTIC NEUTRON SCATTERING

The inelastic neutron scattering measurements were performed on the CRG-IN12 cold neutron 3-axis spectrometer at ILL. The 320 mg sample consisted of two $\text{BaCdVO}(\text{PO}_4)_2$ crystals with 98.8% isotopically enriched ^{144}Cd , co-aligned with a total mosaic of about 10° in the $(h, k, 0)$ scattering plane on an aluminium sample

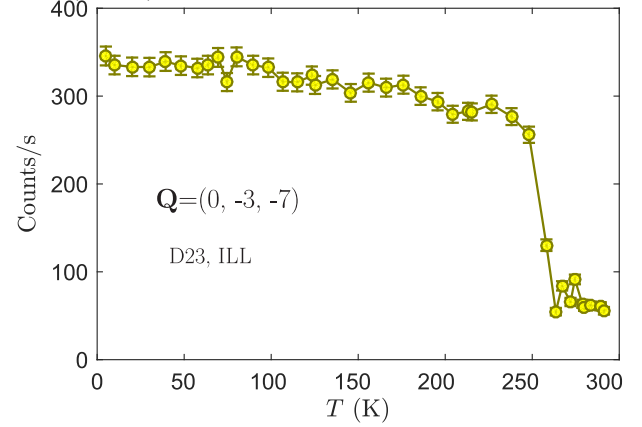


FIG. 1. Temperature dependence of the $(0, -3, -7)$ nuclear Bragg peak intensity obtained at D23 neutron diffractometer (ILL) upon warming. The $(0, -3, -7)$ peak is extinct in P_{bca} structure.

holder. The assembly was mounted on the cold finger of the ^3He - ^4He dilution refrigerator and installed on IN12 with a vertical cryomagnet. The measurements were performed at the base temperature of 70 mK and 10 T magnetic field $\mathbf{H} \parallel \mathbf{c}$. Examples of constant- \mathbf{Q} inelastic scans contributing to the dispersion in Figure 1 of the main text are shown in Fig. 2. The data collected on IN12 are available at <https://doi.ill.fr/10.5291/ILL-DATA.CRG-2577>.

* vvivek@phys.ethz.ch

† zhelud@ethz.ch; <http://www.neutron.ethz.ch/>

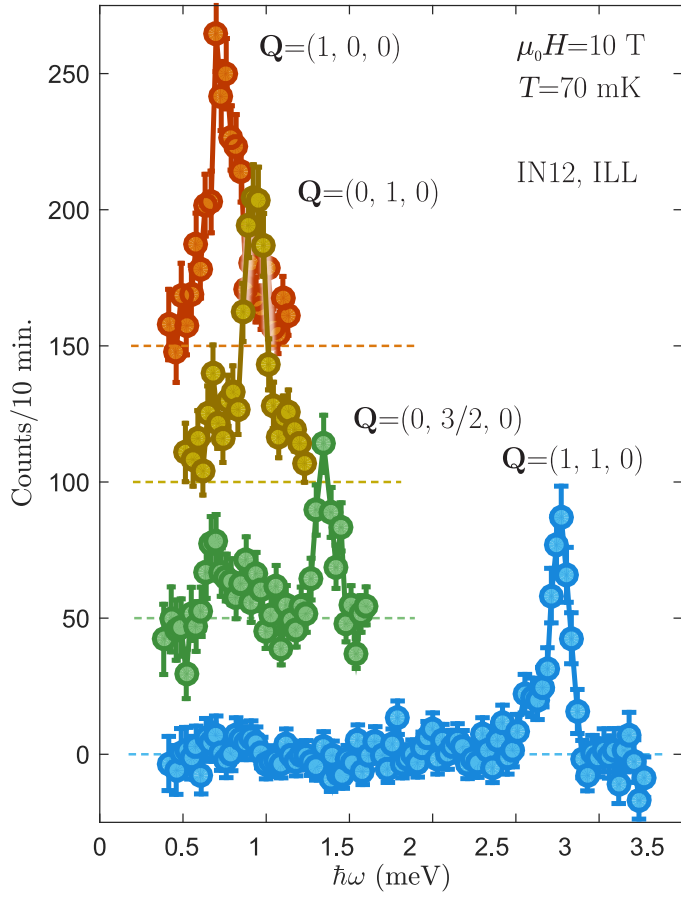


FIG. 2. A few representative, background subtracted, inelastic neutron scattering constant- \mathbf{Q} scans in the fully polarized phase ($10 \text{ T } \mathbf{H} \parallel \mathbf{c}$) of $\text{BaCdVO}(\text{PO}_4)_2$ at 70 mK . An offset of 50 counts/curve is introduced for better visibility and their respective zeroes are indicated by dashed lines.

Lattice parameters	a' (c)	b' (b)	c' (a)
	18.8591(9)	8.8911(4)	8.8621(4)

Symmetry transformations	$P_{ca}2_1$		
	x	y	z
	$-x$	$-y$	$\frac{1}{2} + z$
	$\frac{1}{2} + x$	$-y$	z
	$\frac{1}{2} - x$	y	$\frac{1}{2} + z$

Atom	x	y	z	U_{iso}
Ba 1	0.58655(2)	0.73248(3)	-0.20183(4)	0.00460(4)
Ba 2	0.91837(2)	0.24762(3)	0.43979(4)	0.00465(4)
Cd 1	0.59795(2)	0.60137(4)	0.27429(5)	0.00457(5)
Cd 2	0.41362(2)	0.86375(4)	-0.05557(5)	0.00470(5)
V 1	0.73144(5)	0.39048(9)	0.69354(10)	0.00343(9)
V 2	0.78961(5)	-0.11011(9)	0.69465(10)	0.00317(9)
P 1	0.46975(8)	0.52771(16)	0.04790(18)	0.00401(17)
P 2	0.75096(8)	0.63556(14)	0.44851(19)	0.00289(15)
P 3	0.46817(8)	1.04426(16)	-0.35171(17)	0.00347(17)
P 4	0.74626(8)	0.13737(14)	0.44741(19)	0.00331(16)
O 1	0.4580(2)	0.8816(4)	-0.2934(5)	0.0043(4)
O 2	0.7978(2)	0.5222(4)	0.3610(5)	0.0050(5)
O 3	0.7040(3)	-0.1071(5)	0.7010(6)	0.0080(6)
O 4	0.8029(2)	0.7475(4)	0.5191(5)	0.0053(5)
O 5	0.4614(2)	1.0429(5)	-0.5252(5)	0.0063(5)
O 6	0.5518(2)	0.5426(5)	0.0568(5)	0.0066(5)
O 7	0.8014(2)	0.0598(4)	0.5474(5)	0.0048(4)
O 8	0.4352(3)	0.5629(5)	0.1993(6)	0.0083(6)
O 9	0.4528(2)	0.3614(5)	0.0026(5)	0.0061(5)
O 10	0.7036(2)	0.5575(5)	0.5636(5)	0.0054(5)
O 11	0.6922(2)	0.0299(4)	0.3719(5)	0.0051(5)
O 12	0.6994(2)	0.2489(4)	0.5340(5)	0.0057(5)
O 13	0.4449(2)	0.6250(5)	-0.0881(5)	0.0061(5)
O 14	0.7894(2)	0.2215(4)	0.3268(5)	0.0050(5)
O 15	0.5439(3)	1.0986(5)	-0.3202(6)	0.0085(6)
O 16	0.6995(2)	0.7138(4)	0.3373(5)	0.0046(4)
O 17	0.8167(3)	0.3963(5)	0.6871(6)	0.0078(5)
O 18	0.4097(2)	1.1432(5)	-0.2802(6)	0.0070(5)

TABLE I. Chemical structure of the low-temperature phase of $\text{BaCdVO}(\text{PO}_4)_2$. Correspondence between the axis labels for low- and high temperature structures is shown in brackets.